Recent Performance of and Plasma Outage Studies with the SNS H⁻ Source[a)]

M.P. Stockli[b)], B. Han, S.N. Murray, T.R. Pennisi, C. Piller, M. Santana, R. Welton

Spallation Neutron Source, Oak Ridge National Laboratory, Oak Ridge, Tennessee 37830, USA

(Presented 25 August 2015; received 21 August 2015; accepted XXXXX; published online XXXXX)

SNS ramps to higher power levels that can be sustained with high availability. The goal is 1.4 MW despite a compromised RFQ, which requires higher RF power than design levels to approach the nominal beam transmission. Unfortunately at higher power the RFQ often loses its thermal stability, a problem apparently enhanced by beam losses and high influxes of hydrogen. Delivering as much H^- beam as possible with the least amount of hydrogen led to plasma outages. The root cause is the dense 1-ms long ~55-kW 2-MHz plasma pulses reflecting ~90% of the continuous ~300W, 13-MHz power, which was mitigated with a 4-ms filter for the reflected power signal and an outage resistant, slightly-detuned 13-MHz match. Lowering the H_2 gas also increased the H^- beam current to ~55 mA, and increased the RFQ transmission by ~7% (relative).

I. INTRODUCTION

The SNS (Spallation Neutron Source)[1] Cs-assisted, multicusp, RF (radio frequency) H^- ion source and electrostatic LEBT (low-energy beam transport system) are a part of the front-end that was designed and built by Lawrence Berkeley National Laboratory and delivered to Oak Ridge National Laboratory (ORNL).[2] Over the last twelve years numerous technical and procedural improvements at ORNL brought the source up to the full SNS requirements with record breaking performances.[3-9]

Briefly, as shown in Fig. 1, water-cooled multicusp magnets surround the stainless steel plasma chamber. A 2.5 turn water-cooled, porcelain-coated antenna couples the RF inductively into the high-purity, low-pressure H_2 gas, forming plasma. A set of water-cooled bar-magnets generate a ~300 G transverse magnetic "filter" field which reflects the fast electrons while the slow electrons and ions diffuse towards the outlet. Unaffected by the filter field, rovibrationally excited molecules travel freely to the outlet where they likely form H^- ions when colliding with a slow electron.[10,11] The 7 mm diameter outlet aperture is surrounded by a conical Mo converter which is covered with a partial layer of Cs to enhance the conversion of some of the impacting ions and fast neutrals to H^- ions.[10,12] The partial Cs layer is controlled by keeping the converter at a few hundred °C and by eliminating all impurities because they would sputter the Cs.[13] H^- ions drifting into the meniscus are accelerated by the -65 kV potential of the ion source. A set of 8 "dumping magnets" in the outlet electrode generate a ~1.7 kG dipole field that shoves the co-extracted electrons to the e-dump electrode. The e-dump is kept at +6.2 kV with respect to the ion source to form an uniform extraction field.[4] The two electrostatic lenses refocus the diverging H^- beam into the RFQ (radio frequency quadrupole accelerator) where it is accelerated to 2.5 MeV. Exiting the RFQ the beam passes a beam current monitor (BCM02) which reports the beam current that is optimized because the losses in the linear accelerator are negligible. The LEBT is optically aligned to the RFQ entrance aperture. The deflection of the H^- beam by the dumping magnets can be corrected by tilting the source by ~3°. However, normally more beam is obtained by setting the tilt to 0° and moving the source ~2 mm to the right.[5]

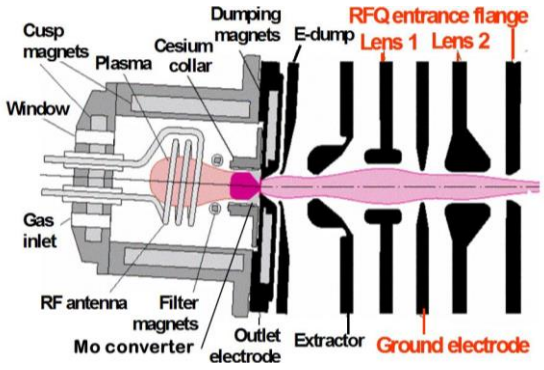

FIG. 1. (Color online) Top view schematic of the SNS H^- source and LEBT.

II. SOURCE PERFORMANCE HISTORY

New technologies and configurations are first tested extensively on the test stand before being introduced on the Frontend. On the other hand, starting up 131 sources on the Frontend for neutron production yielded numerous opportunities for minor procedural changes to improve repeatability and reduce risks of failure.

[a)]Contributed paper published as part of the Proceedings of the 16th International Conference on Ion Source, New York City, NY, August, 2015.
[b)]Author to whom correspondence should be addressed. Electronic mail: stockli@ornl.gov.

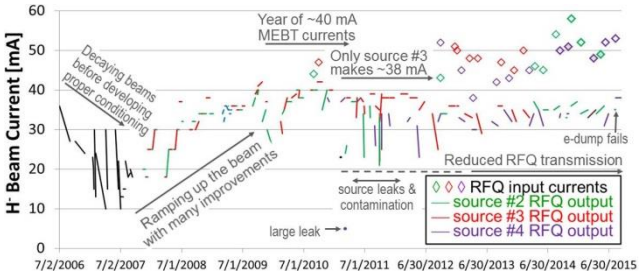

FIG. 2. (Color online). Some RFQ input- and all output-production beam currents.

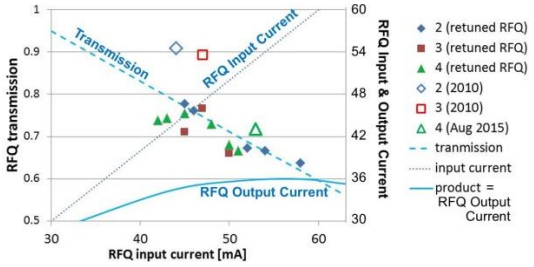

FIG. 3. (Color online). RFQ transmissions, input and output currents versus the RFQ input current.

Figure 2 shows the performance of the 131 sources so far operated for neutron production. A BCM02 bias-corrected measurement at the end of the pulse measured during the first 8 days of service is connected with a line to a measurement taken during the last week of service. Figure 2 shows the first year of decaying beams before proper conditioning was learned.[4,6,13] Then it shows two years of many improvements, which ramped the BCM02 beam to the required 38 mA.[3,4] The ~40 mA performances were maintained for about one year before some degradation became obvious as only one source (#3) could produce 38 mA. Air leaks and a severe contamination compromised the performance even further.[6,7] Finally in 2012 RFQ transmission measurements were reimplemented and showed that the transmission dropped from ~90% in 2010 to ~70%.[8] The RFQ was retuned in summer of 2013, which restored the transmission close to 80%.[8] The diamonds in Fig. 2 show the measured RFQ input currents, which increased 23% since 2010 and 14±6% over the last year while the scatter decreased by ~50%. The last year's improvements are mainly due to more careful tune-ups and retuning throughout the ion source service cycle yielding slight increases compared to slight decreases of the past. It also shows the most recent improvements yielding 38 mA in BCM02 with the current (August 2015) production source (#4), a performance not achieved since early 2011 when the RFQ still had an uncompromised transmission.[6]

III. RFQ TRANSMISSION

Figure 3 shows measured[8] RFQ transmissions only from carefully tuned production ion sources after the RFQ was retuned. The transmission decreases with the beam current injected into the RFQ, which suggests space-charge driven emittance growth in the LEBT because PARMTEQ calculations predict space-charge driven transmission loss only for H^- beam currents above 60 mA.[14] The low-scatter source #2 data suggest a linear decrease as indicated with the dashed line. When this apparent transmission is multiplied with the input current (dotted line) one obtains the expected RFQ output current in the shape of a parabola that peaks near 60 mA input current. This explains why the BCM02 beam currents no longer increase when the RF power is increased beyond ~60 kW, the power typically used to generate the highest H^- beam currents. Figure 3 also shows the two 2010 measurements that were ~15% (absolute) higher. In addition Fig. 3 shows the transmission of the current source (August 2015), which is about 5% (absolute) higher than expected from the linear fit of the source #2 data.

The RFQ transmission can be increased by increasing its RF power.[15] Unfortunately at higher power the RFQ tends to lose its thermal stability, a problem that appears to be enhanced by beam losses and by high influxes of hydrogen. For this reason in March 2014, the high-performing source #3 was demoted to being an emergency spare. Reactivated source #2 claimed the champion position while source #4 continues to serve intermittently as one can see in Fig. 2. Accordingly our goal has shifted to delivering the most H^- beam in the MEBT with the least hydrogen flow. Naturally, this led to many plasma outages that needed to be understood.

IV. THE ION SOURCE RF SYSTEM

Figure 4 shows the ion source RF system. It consists of a grounded low-level 2-MHz generator feeding the grounded 2-MHz QEI amplifier that delivers up to 80-kW at a 6% duty factor into an 2-MHz high voltage transformer.[16] On the ion source high voltage platform is an reconfigurable impedance-matching transformer, which excites the LCR circuit of the aforementioned antenna, enhanced by two 1-µH inductors, which are balanced by a remotely adjustable 2.3 nF vacuum capacitor. A Pearson current monitor 101 reports the antenna current, the most reliable power and performance indicator.

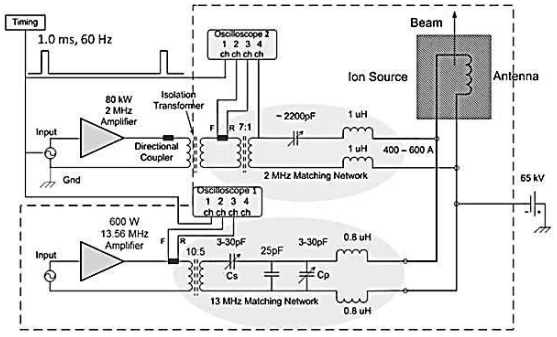

FIG. 4. The 2 and the 13 MHz RF systems powering the plasma antenna.

Also on the ion source high voltage platform is a continuous 600-W 13 MHz RF generator (Comdel CX600) delivering its power to an impedance reducing transformer that drives a 2-capacitor voltage divider, with both capacitors being adjustable. Its output connects through two 0.8 µH inductors to the antenna. In the past the 13 MHz matcher was tuned by minimizing the reflected power indicated by the CX600 before and after striking plasma. Superimposing 2 MHz RF would increase the (average) reflected power, while the optimal tune remained the same. In 2014, to better understand plasma outages, a 13 MHz directional coupler was reactivated and calibrated. Almost immediately the time-resolved data revealed that the 13 MHz tunes were not very consistent.[17] Accordingly 20-turn dials were added to enable systematic studies and to allow for repeatable tunes.

V. PLASMA IGNITION

Plasma ion sources are normally operated below but near the Paschen curve and therefore the plasma is ignited either with a small pressure bump or a large voltage spike as shown in Fig 5. While most low-duty-factor hydrogen sources use easily generated pressure bumps, this technology is unsuitable for our 60 Hz repetition rate. Figure 5 shows that hydrogen is the most difficult gas to ignite, which explains why hydrogen sources are easy to ignite when impurities such as H_2O, N_2, CO, O_2 and CO_2 are present, but become difficult to ignite when the impurities have disappeared after many weeks of continuous operation. Added impurities would sputter the Cesium and cause the decay of the H^- beam current.[6,7] Accordingly most of our plasma studies are either conducted or verified after many weeks of operation at the end of a long ion source service cycle.

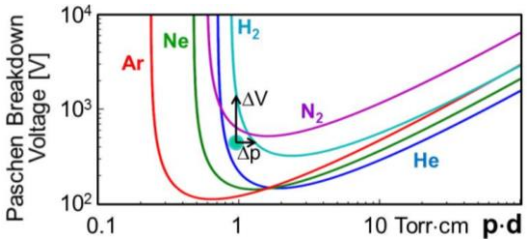

FIG. 5. (Color online). Paschen breakdown voltage versus the pressure-distance product for some gases.

When experiencing plasma outages in 2010 the power of the continuous 13 MHz was raised to 400 W and above. This appeared to cause more outages, and therefore it was returned to the proven 300-350 W. Those outages were finally mitigated by using 1.96 MHz for the first 10 oscillations to compensate for the missing plasma inductance when starting the 2 MHz ~1-ms long RF pulses.[5] In 2013 plasma outages returned when attempting to increase the pulse length from 0.88 to 1.0 ms with old sources. Trying to find a more resonant start frequency, the first 10 oscillations were studied as seen in Fig. 6.

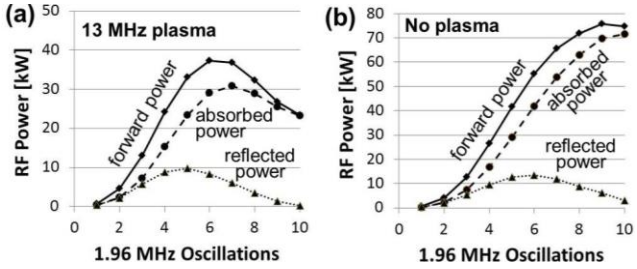

FIG. 6. The first 10 ~2 MHz oscillations (a) with and (b) without continuous 13 MHz plasma.

The data obtained with a 4-week old source show in Fig. 6(a) that the LCR oscillator builds up power rapidly, up to 20 kW within 1 µs. The growing plasma inductance brings the oscillator out of tune causing the forward power to fold back after ~6 oscillations. Most of the power is absorbed and only little is reflected. Figure 6(b) shows the same data taken after a plasma outage: the power grows more rapidly, close to 30 kW within 1 µs. Without the inductance of plasma, the ~2 MHz 80-kW supply delivers up 76 kW of which up to 72 kW are absorbed. Despite the high power, the induced fields are not strong enough to break down the ultra-pure hydrogen gas. The 2 MHz RF needs starter plasma to deliver its energy into the plasma.

Therefore SNS uses a pressure bump to ignite continuous 13 MHz plasma, which is then amplified by the 2 MHz RF to produce the high-current H^- beam pulses. After a plasma outage, the 13 MHz plasma needs to be restarted with a pressure bump. The 2013 plasma outages of the 1-ms long pulses could be eliminated by increasing the start frequency from 1.96 to 1.985 MHz, probably because it better overlaps with the shifting resonance and therefore can absorb more power as seen in Fig. 7.[9]

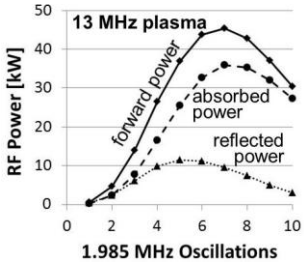

FIG. 7. The first 10 1.985-MHz oscillations amplifying 13 MHz plasma.

VI. PLASMA OUTAGES AND THE 13 MHz RF

Outage data are captured by triggering an oscilloscope with a light detector looking at the plasma. This was done for Fig. 8, which shows the signals from a 2 MHz directional coupler. The first two plasma pulses are characterized by high forward power (top trace) of which only ~4% is reflected (bottom trace). The third pulse has ~50% less forward power of which ~27% is reflected, which is consistent with the oscillator being out of resonance due to the lack of the plasma inductance.

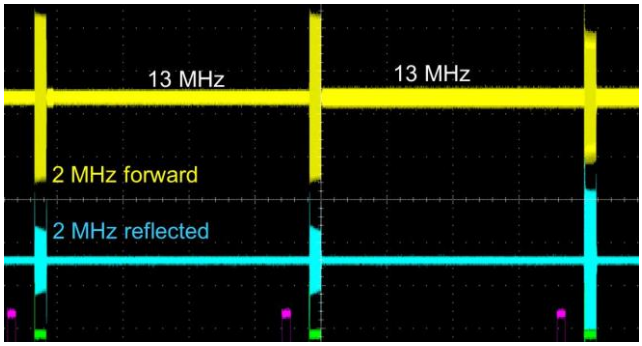

FIG. 8. (Color online). 2 MHz directional coupler data of two beam pulses and an outage.

In between the pulses one sees 13 MHz RF leaking into the 2 MHz coupler, less between the two plasma pulses and more after the second plasma pulse. Apparently the plasma went out right after the second plasma pulse and without absorption by plasma, more 13 MHz is available to leak into the 2 MHz coupler.

The calibration of the 13 MHz directional coupler revealed that while a good tune reflects only a few % of the typical 300 W of 13 MHz power, the reflected power jumps to ~90% during the 2 MHz pulse as seen in Fig 9(a). Many on-resonance and off-resonance tunes were tested without ever seeing much change in the ~90% power reflected by the 2 MHz pulse. The 13 MHz forward power normally does not change during the 2 MHz pulse as seen in Fig. 9(a). The change in reflected power maybe due to a change in resonance as previously concluded from a current measurement.[18] However, the 13 MHz RF may not interact with the entire 2 MHz plasma and/or the highly excited 2 MHz plasma may have no particles that could be readily excited by the 13 MHz RF, and without being able to deliver work, most of the 13 MHz power is reflected.

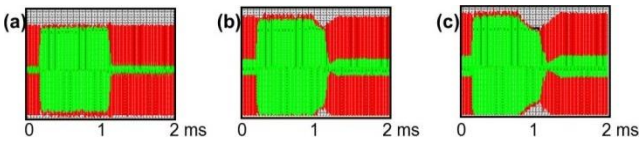

FIG. 9. (Color online). 13 MHz directional coupler data for (a) 300 W, (b) 400W, and (c) 450 W.

The 600-W 13-MHz CX600 has a protection circuit, which folds back its output power to keep the reflected power from exceeding 100W. This is barely noticeable for 300 W shown in Fig. 9(a), but becomes obvious for 400 W shown in Fig. 9(b), where the foldback starts after ~0.7 ms. For 450 W in Fig. 9(c), the foldback starts already after 0.5 ms. With severe foldbacks the thinning plasma can extinguish before the 13 MHz can sufficiently recover.

The rise time of the foldback is governed by a serial 1.2 kΩ resistor in the measured reflected power line, the signal that is compared to the set 100 W limit, and a 0.1 µF feedback capacitor. Increasing the resistor to 3.9 kΩ and the capacitor to 1 µF increases the rise time of the comparator to 4 ms, reducing the averaged power signal by a factor of 4 for the 1 ms long pulses. This allows for up to 400 W reflected power during the 1 ms long pulses without triggering the foldback of the output power as one can see in Fig. 10(a) for 300 W, in Fig. 10(b) for 400 W, and in Fig. 10(c) for 450 W.

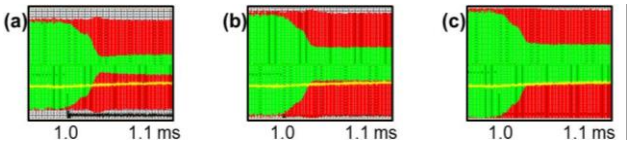

FIG. 10. (Color online). 13 MHz directional coupler data at the end of the 2 MHz pulse for (a) 300 W, (b) 400W, and (c) 450 W.

Operational plasma outages can occur hours after having lowered the H_2 flow or lowered the 13 MHz power, which suggests that there are multiple upsets that contribute, such as voltage upsets. In this work, the robustness of plasma is characterized by slowly lowering the H_2 flow in 0.1 sccm steps and record the last flow before the plasma went out. This method has yielded consistent and repeatable results,[19] although it may lack some of the complexities of operational plasma outages. Figure 11 shows such a study with 300-W 13 MHz forward power and gas flows of 25 sccm in Fig. 11(a), of 20 sccm in Fig. 11(b), and 19.3 sccm in Fig. 11(c). Figures 11(b) and 11(c) show a bulb of reflected power growing before the plasma outage at 19.2 sccm is reached,[19] which appears to be a sign of plasma becoming too thin or too small to readily absorb the 13 MHz power.

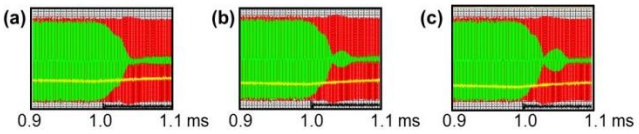

FIG. 11. (Color online). 13 MHz directional coupler data at the end of the 2 MHz pulse for H_2 flows of (a) 25 sccm, (b) 20 sccm, and (c) 19.3 sccm.

Four on-resonance and eight off-resonances tunes are shown in Fig. 12 versus the settings of the two capacitors Cs and Cp shown in Fig. 4. Shown in Fig. 12(a) is the average reflected 13 MHz power, which is the smallest for tunes with low Cs and high Cp, which also produce the brightest plasma as seen in Fig. 12(b) displaying the H-α emission. This was assumed to be the most robust plasma.

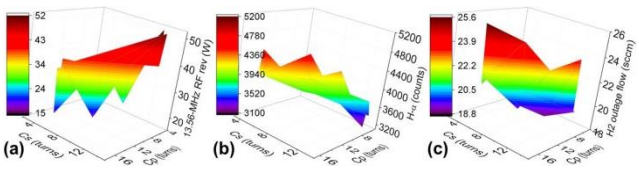

FIG. 12. (Color online). 13 MHz (a) reflected power, (b) H-α emission, and (c) H plasma outage flow versus the tune of Cs and Cp on the right.

Surprisingly the lowest plasma outage flows are found for high Cs and low Cp tunes, as seen in Fig. 12(c), which feature higher reflected power and less H-α emission.[19] Using such a tune allowed for lowering the H_2 flow to 26.5 sccm and produce 38 mA linac beam current within two days of starting up source #4, a performance not achieved for the past 5 years. Even source #3 could not produce such a beam current for the last 2.5 years as seen in Fig. 2. Apparently the reduced H_2 flow reduces the H^- beam divergence and its emittance and so increases its RFQ transmission as seen in Fig. 3.

VII. SOURCE SERVICE CYCLES AND LIFETIMES

Since the beginning of the first production run in 2012 through today, 33 H^- sources were started up on the SNS Frontend for neutron production. Of those 33 sources 2 had to be replaced prematurely because an e-dump insulator failed within the first five days as shown in Fig. 13. The e-dump is in a precarious position because when the e-dump arcs to the nearby extractor, its voltage with respect to the source can raise drastically above its specification. Several times, the e-dump insulators have been made more robust and that effort continues. In addition a fast bleed resistor will be added to better control such voltage spikes.

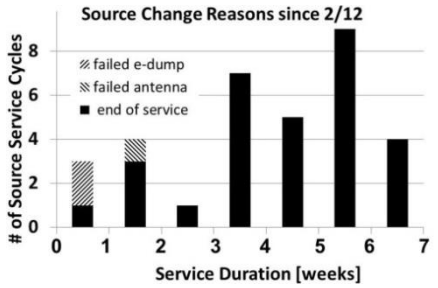

FIG. 13. The SNS H^- source service cycle and failure statistics.

Only 1 source had to be replaced very early in 2013 when an antenna failed after 11 days of operation. More frequent antenna failures encountered in 2010 and 2011 were caused by a combination of 7.2% ion source conditioning, thicker antenna coatings, insufficient cleanliness in manufacturing, and a lack of quality control and assurance.[11] In the meantime, the manufacturer has improved the cleanliness of the fabrication in several steps, the coating has been reduced to between 0.4 and 0.5 mm, and the received antenna are inspected for imperfections.

Since a while the diameter of the antenna section that is subjected to the highest plasma pressure is measured before and after its service cycle. An average wear of 44 μm was found, about 10% of the coating. The measured wear is plotted against its service duration in Fig. 14 and shows practically no correlation with a correlation coefficient of 0.12. This is consistent with the lack of old age failures in Fig. 13 and with spectroscopic plasma emission observations.[17] Accordingly the H^- source service cycle is being extended to ~10 weeks, during which the source has to deliver ~5 A·h of H^- into the RFQ.

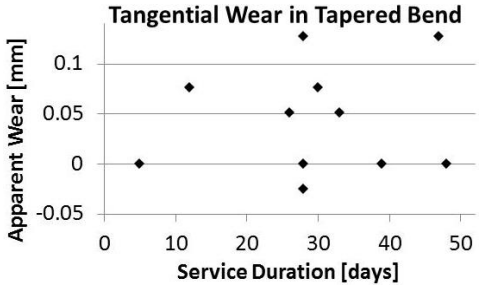

FIG. 14. Apparent antenna wear versus service duration.

ACKNOWLEDGMENT

SNS is indebted to LBNL for delivering the highly capable SNS front end. We also acknowledge various contributions from numerous SNS colleagues, who contributed to this success, including the proofreading by J. Homes. Work was performed at Oak Ridge National Laboratory, which is managed by UT-Battelle, LLC, under contract DE-AC05-00OR22725 for the U.S. Department of Energy.

[1]S. Henderson et al, Nucl. Instrum. Meth. **A763,** 610-673 (2014).
[2]R. Keller, R. Thomae, M. Stockli, R. Welton, AIP Conf. Proc. **639**, 47 (2002).
[3]M.P. Stockli, B.X. Han, S.N. Murray, D. Newland, T.R. Pennisi, M. Santana, R.F. Welton, AIP Conf. Proc. **1097**, 223 (2009).
[4]M.P. Stockli, B. Han, S.N. Murray, T.R. Pennisi, M. Santana, R.F. Welton, Rev. Sci. Instrum. **81**, 02A729 (2010).
[5]B. Han, T. Hardek, Y.W. Kang, S.N. Murray, T.R. Pennisi, C. Piller, M. Santana, R.F. Welton, M.P. Stockli, AIP Conf. Proc. **1390**, 216 (2011).
[6]M.P. Stockli, B.X. Han, T.W. Hardek, Y.W. Kang, S.N. Murray, T.R. Pennisi, C. Piller, M. Santana, R.F. Welton, Rev. Sci. Instrum. **83**, 02A732 (2012).
[7]M.P. Stockli, B.X. Han, S.N. Murray, T.R. Pennisi, M. Santana, R.F. Welton, AIP Conf. Proc. **1515**, 292 (2013).
[8]M.P Stockli, K.D. Ewald, B.X. Han, S.N. Murray, Jr., T.R. Pennisi, C. Piller, M. Santana, J. Tang, R. Welton, Rev. Sci. Instrum. **85**, 02B137 (2014).
[9]M.P. Stockli, B.X. Han, S.N. Murray, T.R. Pennisi, C. Piller, M. Santana, R.F. Welton, AIP Conf. Proc. **1655**, 030001 (2015).
[10]M. Bacal and M. Wada, Appl. Phys. Rev. **2**, 021305 (2015).
[11]M.P. Stockli, CERN Report CERN-2013-7, 265 (2013).
[12]M.P. Stockli, J. of Phys. Conf. Ser. **399**, 012001 (2012).
[13]M.P. Stockli, B.X. Han, S.N. Murray, T.R. Pennisi, M. Santana, R.F. Welton, AIP Conf. Proc. **1390**, 123 (2011).
[14]A. Aleksandrov, Spallation Neutron Source, Oak Ridge, TN 37830, USA, private communication (2006).
[15]A.P. Shishlo, Spallation Neutron Source, Oak Ridge, TN 37830, USA, private communication (2013).
[16]Y.W. Kang, R. Fuja, R.H. Goulding, T. Hardek, S.W. Lee, M.P. McCarthy, M.C. Piller, K. Shin, M.P. Stockli, R.F. Welton, Rev. Sci. Instrum. **81**, 02A725 (2010).
[17]B. Han, M.P. Stockli, R.F. Welton, S.N. Murray Jr., T.R. Pennisi, M. Santana, AIP Conf. Proc. **1655**, 030003 (2015).
[18]T. Schenkel, J.W. Staples, R.W. Thomae, J. Reijonen, R.A. Gough, K.N. Leung, R. Keller, R. Welton, and M. Stockli, Rev. Sci. Instrum. **73**, 1017 (2002).
[19]B. Han, M.P. Stockli, Y. Kang, S.N. Murray Jr., T.R. Pennisi, M. Santana, R.F. Welton, these proceedings.